

# Total Cross-Section Measurement and Diffractive Physics with TOTEM

*M. Deile on behalf of the TOTEM Collaboration*  
CERN, Genève, Switzerland

## Abstract

The TOTEM Experiment will measure the total pp cross-section and study elastic and diffractive scattering at the LHC. For the initial LHC running period, TOTEM has requested a beam optics with  $\beta^* = 90$  m which fits well into the standard LHC start-up scenario and whose commissioning is expected to be less complex than the one of TOTEM's baseline optics with  $\beta^* = 1540$  m. The early running conditions will allow a measurement of the total pp cross-section and – independently – of the luminosity at the 5% level. In addition, the cross-sections and topologies of soft diffractive events can be studied. At a later stage, the precision of the total and elastic cross-section measurements will be improved to the 1% level by using the final TOTEM optics, and the diffraction studies will be extended by collaborating with CMS.

## 1 Introduction

The TOTEM apparatus [1] with its unique coverage of high rapidities ( $3.1 \leq |\eta| \leq 6.5$ ) and with its unprecedented acceptance for surviving protons is the ideal tool for studying forward phenomena, including elastic and diffractive scattering. Since the particle multiplicity of inelastic events (both non-diffractive and diffractive) peaks in the forward region (Figure 1), TOTEM accepts about 95 % of all inelastic events in its trigger. This is crucial for achieving TOTEM's main objective for the first years of LHC operation, the luminosity-independent measurement of the total cross-section based on the Optical Theorem.

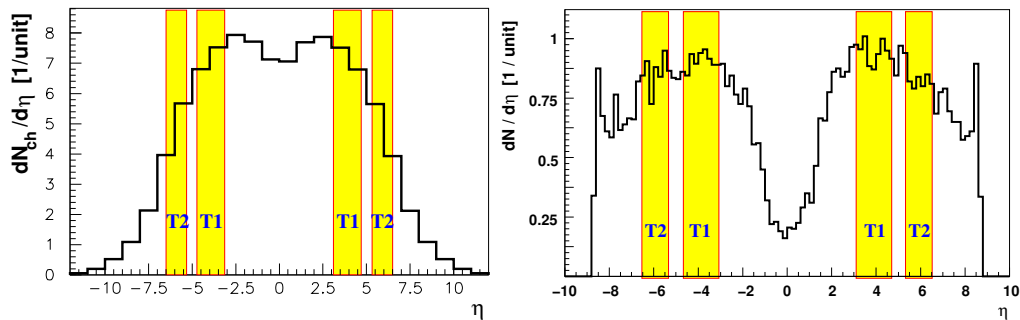


Fig. 1: Pseudorapidity distributions of the charged particle multiplicity for non-diffractive (left) and single diffractive, SD, (right) inelastic collisions at 14 TeV.

## 2 Measurement of the Total pp Cross-Section

### 2.1 Motivation and Technique

A precise measurement of the total pp cross-section  $\sigma_{tot}$  and of the elastic scattering over a large  $t$ -range is of primary importance for distinguishing between different models of soft proton interactions.

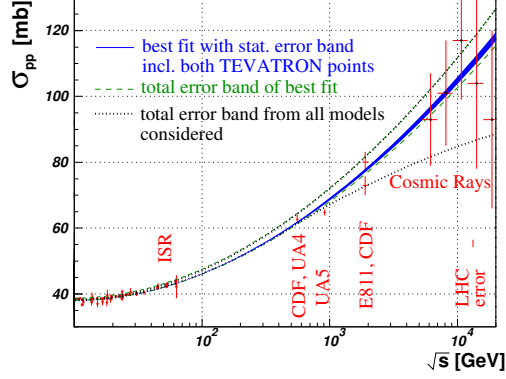


Fig. 2: COMPETE fits [2] to all available  $pp$  and  $p\bar{p}$  scattering data with statistical (blue solid) and total (green dashed) error bands, the latter taking into account the Tevatron ambiguity. The outermost curves (dotted) give the total error band from all parameterisations considered.

Figure 2 summarises the existing measurements of  $\sigma_{tot}$  from low energies up to collider and cosmic-ray energies. Taking into account all available data, the COMPETE collaboration [2] has performed fits of the energy dependence of the total cross-section and the ratio  $\rho$  of the real to imaginary parts of the elastic scattering amplitude, based on different models. The model leading to the best fit predicts for the LHC at  $\sqrt{s} = 14$  TeV:

$$\sigma_{tot} = 111.5 \pm 1.2^{+4.1}_{-2.1} \text{ mb}, \quad \rho = 0.1361 \pm 0.0015^{+0.0058}_{-0.0025}, \quad (1)$$

where the second error is due to the 2.6 standard-deviations discrepancy between the two final results from TEVATRON [3,4]. The cosmic-ray data with their large uncertainties do not provide strong constraints on the model choice. Inclusion of the full set of COMPETE's models leaves a wide range for the expected value of  $\sigma_{tot}$  at 14 TeV, typically from 90 to 130 mb.

The total  $pp$  cross-section is related to nuclear elastic forward scattering via the two relations

$$\mathcal{L} \sigma_{tot}^2 = \frac{16\pi}{1 + \rho^2} \cdot \left. \frac{dN_{el}}{dt} \right|_{t=0} \quad \text{and} \quad \mathcal{L} \sigma_{tot} = N_{el} + N_{inel}, \quad (2)$$

the first of which is known as the Optical Theorem. This equation system can be resolved for  $\sigma_{tot}$  or  $\mathcal{L}$  independently of each other:

$$\sigma_{tot} = \frac{16\pi}{1 + \rho^2} \cdot \frac{dN_{el}/dt|_{t=0}}{N_{el} + N_{inel}}, \quad (3)$$

$$\mathcal{L} = \frac{1 + \rho^2}{16\pi} \cdot \frac{(N_{el} + N_{inel})^2}{dN_{el}/dt|_{t=0}}. \quad (4)$$

Hence the quantities to be measured are the following:

- $dN_{el}/dt|_{t=0}$ : The nuclear part of the elastic cross-section extrapolated to  $t = 0$  (see Section 2.3). The expected uncertainty of the extrapolation depends on the acceptance for elastically scattered protons and hence on the beam optics.
- The total nuclear elastic rate  $N_{el}$  measured by the Roman Pot system and completed by the extrapolation of the nuclear part  $dN_{el}^{nuc}/dt$  to  $t = 0$ .
- The inelastic rate  $N_{inel}$  consisting of diffractive ( $\sim 18$  mb at LHC) and minimum bias ( $\sim 65$  mb at LHC) events. It will be measured by the tracking stations T1 and T2.

For the rate measurements it is important that all TOTEM detector systems have level-1 trigger capability. The parameter  $\rho = \frac{\mathcal{R}[f_{el}(0)]}{\mathcal{I}[f_{el}(0)]}$ , where  $f_{el}(0)$  is the forward nuclear elastic amplitude, has to be taken from external theoretical predictions, e.g. [2]. Since  $\rho \sim 0.14$  enters only in a  $1 + \rho^2$  term, its impact is small. At a later stage of TOTEM operation, a measurement of  $\rho$  via the interference between Coulomb and nuclear contributions to the elastic scattering cross-section might be attempted at a reduced centre-of-mass energy of about 8 TeV [5].

## 2.2 Inelastic Rate

The measurement of the inelastic rate is based on inclusive triggers with the forward trackers T1 and T2 and the Roman Pots. To maximise the event detection efficiency on one hand and to optimise the separation of physics signals from machine background on the other hand, an interplay of various trigger strategies will be adopted:

- The inelastic single-arm trigger (requiring activity in T1 or T2 on one side of the IP) has the best efficiency, missing only events with very low diffractive masses ( $< 10$  GeV for SD). However, it suffers from beam-gas background.
- The inelastic double-arm trigger (requiring activity in T1 or T2 on both sides of the IP) suppresses beam-gas background by its coincidence requirement. However, it cannot be used for single diffraction and suffers from reduced efficiency in low-mass double diffraction.
- The purity of the inelastic triggers can be enhanced by reconstructing the interaction vertex from the tracks in T1 or T2.
- Triggering on “non-colliding bunch crossings”, where the bunch position in one beam is empty, gives access to a direct measurement of the beam-gas background rate which can then be statistically subtracted from the data obtained with normal triggers.
- Single Diffractive and Double Pomeron Exchange events can be tagged by supplementing the inelastic trigger with a proton trigger on one or both sides of the Roman Pot spectrometer. However, proton inefficiencies in a small kinematic region with low values of  $|t|$  have to be extrapolated in this trigger scheme.
- The rates of low-mass single or double diffractive events which are missed in all trigger schemes can be statistically recovered by extrapolating the measured cross-section under theoretical assumptions on  $\frac{d\sigma}{dM^2}$ . However, one has to keep in mind that low-mass resonances typically escape such extrapolations.

The result of the trigger loss estimate (see [1,5]) is 0.8 mb or 1% of the predicted inelastic cross-section of 80 mb.

### 2.3 Elastic Scattering

The determination of total cross-section and luminosity according to Eqns. (3) and (4) requires two aspects of elastic scattering to be measured: the total elastic rate and the extrapolation of the differential cross-section  $d\sigma/dt$  to the Optical point  $t = 0$ . Obviously, to be complete, the measured elastic rate has to be complemented by the extrapolated part, so that this extrapolation enters twice in the procedure.

With the  $\beta^* = 90$  m optics [5], protons with  $|t| > 0.03 \text{ GeV}^2$  are observed in the RP detector at 220 m. This acceptance starting point lies well above the region where the delicate effects from the interference between nuclear and Coulomb scattering play a role. Hence no such perturbation needs to be included in the extrapolation procedure, in contrast to the final  $\beta^* = 1540$  m optics with  $|t|_{\min} = 10^{-3} \text{ GeV}^2$ .

Most theoretical models [6] predict an almost exponential behaviour of the cross-section up to  $|t| \approx 0.25 \text{ GeV}^2$ , as shown in Figure 3. The deviations from a purely exponential shape are quantified by the exponential slope  $B(t) = \frac{d}{dt} \ln \frac{d\sigma}{dt}$  in Figure 3 (right). For all the models considered – except for the one by Islam et al. – the deviations are small. In the  $t$ -range mentioned, the slope  $B(t)$  can be well described by a parabola which is therefore used for the fitting function and the extrapolation. Since this quadratic behaviour of the slope characterises all the models, the extrapolation method is valid in a model-independent way.

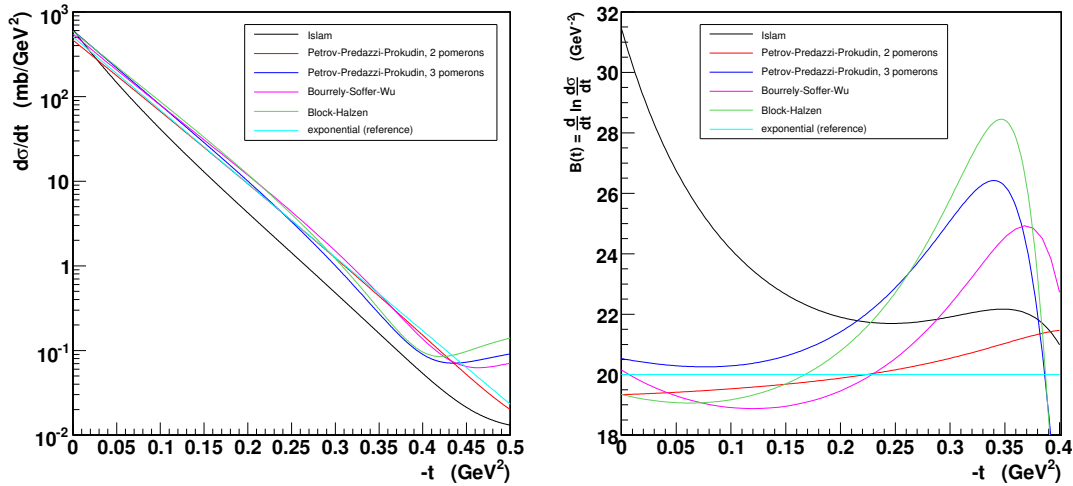


Fig. 3: Left: Differential cross-section of elastic scattering at 14 TeV as predicted by various models. Right: Exponential slope of the differential cross-section.

With the  $\beta^* = 90$  m optics – on which we will focus in all the following considerations – the effective length  $L_x$  (220 m) at the Roman Pot at 220m is 0. Hence in this station only the  $y$ -component of the scattering angle is measured and only the  $t_y \equiv t \sin^2 \varphi \approx (p \Theta_y^*)^2$  component reconstructed. Using the azimuthal symmetry of the elastic scattering process and hence the equality of the distributions of  $t_y$  and  $t_x$ , the distribution  $d\sigma/dt$  can be calculated from  $d\sigma/dt_y$  distribution.

The accuracy of the simulated extrapolation is shown in Figure 4. The key contributions

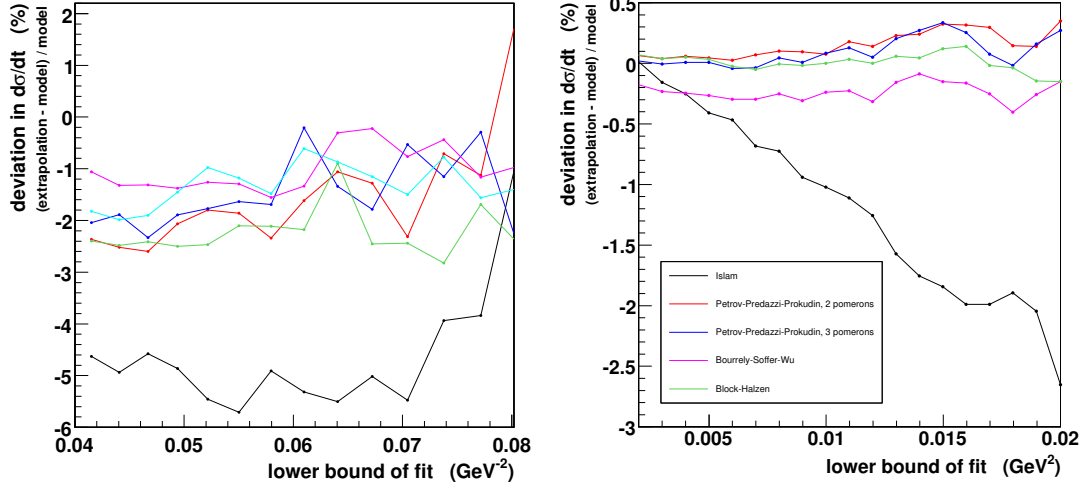


Fig. 4: Extrapolation results based on a MC simulation (not including the  $L_{eff}$  error). Left:  $\beta^* = 90$  m, right:  $\beta^* = 1540$  m for comparison. The  $t_y$ - ( $t$ -) distributions were fitted from the indicated lower bound to  $0.25 \text{ GeV}^2$  ( $0.025 \text{ GeV}^2$ ) respectively.

are the following:

- Smearing effects of the  $t$ -measurement which are dominated by the beam divergence ( $\sigma_{beam} = 2.3 \mu\text{rad}$ ). Based on our preliminary MC simulations this contribution leads to a shift of  $-2\%$  in the extrapolation result (Figure 4 left).
- The statistical error of the extrapolation for an integrated luminosity of  $2 \text{ nb}^{-1}$  corresponding to  $2 \times 10^4 \text{ s}$  (about 5 hours) of running at a luminosity of  $10^{29} \text{ cm}^{-2} \text{ s}^{-1}$ .
- Systematic uncertainty of the  $t$ -measurement: the dominant contribution comes from the uncertainty of the effective length  $L_{eff}$ . The expected precision of  $2\%$  would lead to an extrapolation offset of about  $3\%$ .  
Due to the thick beam at  $\beta^* = 90 \text{ m}$  ( $\sigma_{y_{beam}} = 625 \mu\text{m}$  at RP220) compared to  $\beta^* = 1540 \text{ m}$  ( $\sigma_{y_{beam}} = 80 \mu\text{m}$ ), detector or beam position inaccuracies have a much smaller impact on the  $t$  measurement.
- Model-dependent deviations of the nuclear elastic pp cross-section from an exponential shape lead to a bias in the extrapolation (left-hand plot in Figure 4). Besides the Islam model which can be excluded or confirmed by the measured  $t$ -distribution at large  $t$ -values, the models stay within  $\pm 1\%$ .

## 2.4 Combined Measurement Uncertainty

For the early TOTEM optics with  $\beta^* = 90 \text{ m}$ , the total uncertainty of  $\sigma_{tot}$  in Eqn. (3) has the following contributions:

- Inelastic rate:  $\frac{\delta(N_{inel})}{N_{inel}} \approx 1\%$ . This contribution is almost independent from the beam optics, exceptions being SD and DPE where for some trigger strategies leading protons are parts of the signature.
- Extrapolation of the elastic cross-section: For the early TOTEM optics with  $\beta^* = 90 \text{ m}$ ,  $\frac{\delta(dN_{el}/dt|_{t=0})}{dN_{el}/dt|_{t=0}} \leq 4\%$ .

- Elastic rate: For  $\beta^* = 90$  m,  $\frac{\delta(N_{el})}{N_{el}} \leq 2\%$ . The high correlation between  $N_{el}$  and  $\frac{\delta(dN_{el}/dt|_{t=0})}{dN_{el}/dt|_{t=0}}$  leads to a partial cancellation of errors, which is taken into account in the error combination below.
- The  $\rho$  parameter, estimated to be about 0.14 by extrapolating measurements at lower energies [2], enters  $\sigma_{tot}$  in the factor  $\frac{1}{1+\rho^2} \sim 0.98$ , and hence gives only a relative contribution of about 2%. Assuming a relative uncertainty of 33% on  $\rho$ , determined by the error of the measurements at TEVATRON [4] and extrapolation to LHC energies, we expect an uncertainty contribution of  $\frac{\delta(1+\rho^2)}{1+\rho^2} = \begin{smallmatrix} +1.4\% \\ -1.2\% \end{smallmatrix}$ .

Combination of all these uncertainties by error propagation taking into account the correlations yields a relative error of 4% in  $\sigma_{tot}$ . The uncertainty of the luminosity calculated from Eqn. (4) is slightly worse (7%) because the total rate enters squared.

At a later stage, the final baseline optics with  $\beta^* = 1540$  m will allow a precision improvement to the 1% level. However, to achieve this ambitious goal, an improved knowledge of the optical functions and a RP alignment precision better than  $50 \mu\text{m}$  will be needed.

### 3 Soft Diffraction

Fig. 5 (left) shows the  $(t, \xi)$  acceptances integrated over  $\varphi$  for the special TOTEM optics ( $\beta^* = 90$  m and 1540 m) and for the low- $\beta^*$  optics (2 m is shown, 0.5 m and 11 m are similar). While for  $\beta^* = 0.5$  m only protons with  $\xi > 2\%$  – corresponding to rather high diffractive masses – are observed, the TOTEM optics give access to all  $\xi$ -values down to  $10^{-8}$ , except for very low  $|t|$ -values. Consequently, a large fraction of the diffractive protons is observed: 65% for  $\beta^* = 90$  m and 95% for 1540 m, allowing first measurements of SD and DPE at LHC. Due to the vanishing effective length  $L_x$  at RP220 for the  $\beta^* = 90$  m optics, the dependence of the  $x$ -position on the emission angle  $\Theta_x^*$  is eliminated, which leads to a  $\xi$ -resolution of  $6 \times 10^{-3}$ , mainly due to the vertex uncertainty. For  $\xi < 6 \times 10^{-3}$  where  $\sigma(\xi)/\xi > 100\%$ , events will rather be reconstructed via their rapidity gap (Fig. 5, right). In the regions  $0.0017 < \xi < 0.045$  and  $1 \times 10^{-7} < \xi < 3 \times 10^{-6}$ , the gap edge lies within the acceptance of one arm of T1 or T2, resulting in a resolution of  $\sigma_{\Delta\eta}(\xi)/\xi = 0.8 \div 1$ . At a later stage, joint data taking together with CMS [7] will benefit from a complete rapidity gap acceptance in the range  $3.1 < \Delta\eta < 16.1$ . Furthermore, vertex reconstruction by CMS with an accuracy of  $30 \mu\text{m}$  will improve the  $\xi$ -resolution to  $1.6 \times 10^{-3}$ .

### References

- [1] TOTEM: Technical Design Report, CERN-LHCC-2004-002; addendum CERN-LHCC-2004-020.
- [2] J.R. Cudell et al.; Benchmarks for the Forward Observables at RHIC, the Tevatron-Run II, and the LHC; PRL **89**, (2002) 201801.
- [3] CDF Collaboration (F. Abe et al.), Phys. Rev. **D 50**, (1994) 5550.
- [4] E710 Collaboration (N.A. Amos et al.), PRL **63**, (1989) 2784; Phys. Lett. **B 243**, (1990) 158.  
E811 Collaboration (C. Avila et al.), Phys. Lett. **B 445**, (1999) 419; Phys. Lett. **B 537**, (2002) 41.
- [5] TOTEM collaboration: TOTEM Physics, Proceedings of 17th Rencontre de Blois: 11th International Conference on Elastic and Diffractive Scattering, Château de Blois, France, 2005. arXiv: hep-ex/0602025.
- [6] M. M. Islam, R. J. Luddy and A. V. Prokudin: Near forward pp elastic scattering at LHC and nucleon structure, Int. J. Mod. Phys. A21 (2006) pp. 1–42.

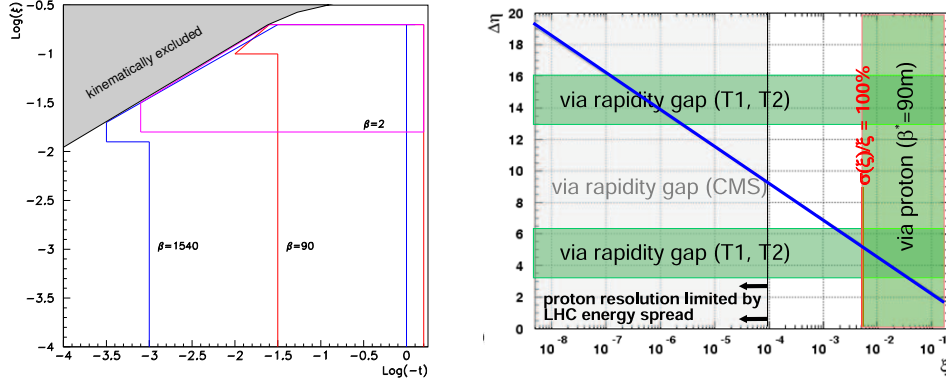


Fig. 5: Left: Acceptance in  $\log_{10} t$  and  $\log_{10} \xi$  for diffractive protons at RP220 for different optics. The contour lines represent the 10 % level. Right: Rapidity gap as a function of  $\xi$  (diagonal line). In the shaded regions TOTEM can reconstruct events via protons (vertical band) or via the rapidity gap in T1 or T2 (horizontal bands).

Claude Bourrely, Jacques Soffer, and Tai Tsun Wu: Impact-picture phenomenology for  $\pi^+ p$ ,  $K^+ p$  and  $p p$ , anti- $p p$  elastic scattering at high energies, Eur. Phys. J. C28 (2003), pp. 97–105.

V. A. Petrov, E. Predazzi and A. Prokudin: Coulomb interference in high-energy  $p p$  and anti- $p p$  scattering, Eur. Phys. J. C28 (2003) pp. 525–533.

M. M. Block, E. M. Gregores, F. Halzen and G. Pancheri: Photon proton and photon photon scattering from nucleon nucleon forward amplitudes, Phys. Rev. D60 (1999) 054024.

- [7] The CMS and TOTEM diffractive and forward working group: Prospects for Diffractive and Forward Physics at the LHC, CERN/LHCC 2006-039/G-124, 2006.